Vol 15 No 12, December 2006
1009-1963/2006/15(12)/2819-09

Chinese Physics

© 2006 Chin. Phys. Soc.
and IOP Publishing Ltd

A method of solving the stiffness problem in Biot's poroelastic equations using a staggered high-order finite-difference*

Zhao Hai-Bo(赵海波)[a)†], Wang Xiu-Ming(王秀明)[a)b)], and Chen Hao(陈 浩)[a)]

[a)] *Institute of Acoustics, Chinese Academy of Sciences, Beijing* 100080, *China*
[b)] *Australian Resources Research Centre, Australian Commonwealth Scientific and Industrial Research Organization, Bentley WA* 6102, *Australia*

(Received 13 April 2006; revised manuscript received 29 April 2006)

In modelling elastic wave propagation in a porous medium, when the ratio between the fluid viscosity and the medium permeability is comparatively large, the stiffness problem of Biot's poroelastic equations will be encountered. In the paper, a partition method is developed to solve the stiffness problem with a staggered high-order finite-difference. The method splits the Biot equations into two systems. One is stiff, and solved analytically, the other is nonstiff, and solved numerically by using a high-order staggered-grid finite-difference scheme. The time step is determined by the staggered finite-difference algorithm in solving the nonstiff equations, thus a coarse time step may be employed. Therefore, the computation efficiency and computational stability are improved greatly. Also a perfect by matched layer technology is used in the split method as absorbing boundary conditions. The numerical results are compared with the analytical results and those obtained from the conventional staggered-grid finite-difference method in a homogeneous model, respectively. They are in good agreement with each other. Finally, a slightly more complex model is investigated and compared with related equivalent model to illustrate the good performance of the staggered-grid finite-difference scheme in the partition method.

Keywords: porous media, stiffness, partition method, staggered grid, finite difference

PACC: 0340K, 4320, 9130

1. Introduction

Recently, the studies of the acoustic properties of porous media in geophysics have received increasing attention. Hydrocarbon reservoirs are composite multiphase media with gas or liquid or both contained in pores of the porous media. It is well known that understanding elastic wave propagation in such a medium is of crucial importance in geophysical exploration and reservoir engineering. Efforts have been made to apply acoustic methods to evaluating and characterizing hydrocarbon reservoirs and to monitoring reservoir production in enhancing oil recovery processes. Numerical simulation has been combined with the theory of elastic waves for Biot's two-phase model in understanding and interpreting the seismic and borehole wave characteristics.[1−5] Based on continuum mechanics and macroscopic constitutive equations, Biot[6−8] developed a theory of wave motion in porous elastic solids with fluid-filled pores for the first time. Many authors[9−11] have made their contributions to Biot's theory. Based on the theory, in addition to the regular P wave and S wave, a slow P wave, which arises from the relative motion between the solid and the fluid, may be present in a porous.

For a complex geological model, generally, it is not possible to obtain analytical solutions to Biot's equations. We can use numerical methods to solve the wave propagation problem in such a porous model. There are three major methods used in modelling seismic wave propagation, i.e. the finite difference (FD) method, the finite element (FE) method including a boundary element (BE) method, and the pseudo-spectral (PS) method. Each of these methods has its own advantages and disadvantages, depending on physical models of interests. For the FD method, there are also various technologies to conduct numerical discretization, such as the Runge–Kutta, Lax–Wendroff, and staggered FDs, and rotated staggered FD methods.

In general, a dynamical equation system has the form of $\dot{S} = US$, where S is the wave field vector,

*Project supported by the "100 Talents Project" of the Chinese Academy of Sciences and the Major Program of the National Natural Science Foundation of China (Grant No 10534040).
†E-mail: zhaohaibo1019@126.com

U is the propagation matrix, and the dot represents time differentiation. For Biot's poroacoustic system, all the eigenvalues of the propagation matrix have negative real part, and the matrix has a relatively large eigenvalue.[12] A stiff system of equations is one for which the maximum eigenvalue of absolute amplitude of the amplification matrix is enormous, so that either the stability or the error bound or both can only be assured by unreasonable restriction on a temporal step. Thus an excessively small step requires too many iterative times in solving the numerical problem.[13] In this way, the system of Biot's poroacoustic differential equations is stiff. As in poroacoustic case, the poroelastic equations system is also stiff.[14] Carcione[12] proposed a partition method in Biot's poroacoustic and poroelastic equations to solve the stiffness problem. The stiff part is solved analytically, and the nonstiff part by Runge-Kutta (R-K) algorithm in time domain and PS method in space domain.

In this paper, the partition method is employed to settle the stiffness problem of Biot's poroelastic equations. For the nonstiff set of equations, instead of using the pseudo spectral method, we use the higher-order stagger-grid FD method to obtain the numerical solutions. The reason why we do not use the PS method as is done in Ref.[12,14] is because the PS method generates strong artificial waves due to its infinitive differential operator for strong impedance contrast. More detailed studies on this issue are seen in Ref.[4]. Also, based on our previous work,[15,16] a perfectly matched layer (PML) technology is used as absorbing boundary condition (ABC) to avoid artificial reflections at the boundaries of the discrete model.

2. Biot's dynamical equations

The dynamical equations describing wave propagation in a heterogeneous porous medium are given by Biot who considered the viscous coupling between solid matrices and pore fluids, and energy dissipation due to the relative motion between the solids and the fluids. For a statistically isotropic, locally homogeneous, porous elastic medium fully saturated by one fluid, if the pores are connected with each other, and only the problem is linear, Biot's dynamical governing equations are[7,8]

$$\dot{\sigma}_{ij} = 2\mu\dot{e}_{ij} + \left[(A+Q)\,\dot{e} - Q\dot{\xi}/\phi\right]\delta_{ij}, \tag{1a}$$

$$\dot{\sigma} = [(Q+R)\dot{e} - R\dot{\xi}/\phi], \tag{1b}$$

$$\dot{v}_i^{\mathrm{s}} = R_1\sigma_{,i} - R_2\sigma_{ij,j} + bR_3 v_i^{\mathrm{f}}, \tag{2a}$$

$$\dot{v}_i^{\mathrm{f}} = -R_3\sigma_{ij,j} + S_1\sigma_{,i} + bS_2 v_i^{\mathrm{f}}, \tag{2b}$$

where σ_{ij} is the stress tensor of the solid; σ is the stress of the fluid; $e_{ij} = [(\partial u_j^{\mathrm{s}}/\partial x_i + \partial u_i^{\mathrm{s}}/\partial x_j)/2]$ is the strain tensor of the solid; $\xi = \phi\nabla\cdot(\boldsymbol{u}^{\mathrm{s}} - \boldsymbol{u}^{\mathrm{f}})$ is the dilatation for the relative motion between the fluid and the solid; $\boldsymbol{u}^{\mathrm{s}}$ is the particle displacement vector of the solid; $\boldsymbol{u}^{\mathrm{f}}$ is the particle displacement vector of the fluid; v_i^{s} is the particle velocity components of the solid; v_i^{f} is the particle-velocity components of the fluid; μ is the shear modulus of the dry porous matrix of interest; $e = \sum e_{ii}$; ϕ is the medium porosity; δ_{ij} is the Kronecker's delta function; A, Q and R are Biot's elastic parameters; b is the damping coefficient denoted by $\phi^2\eta/\kappa$; η is fluid viscosity; κ is the permeability of the porous medium. In the above equations, the dots above the variables represent the derivative with respect to time. The coefficients mentioned in Eqs.(1) and (2) are written as

$$\begin{aligned}
R_1 &= \rho_{12}/(\rho_{12}^2 - \rho_{11}\rho_{22}),\\
R_2 &= \rho_{22}/(\rho_{12}^2 - \rho_{11}\rho_{22}),\\
R_3 &= (\rho_{12} + \rho_{22})/(\rho_{12}^2 - \rho_{11}\rho_{22}),\\
S_1 &= (\rho_{11} + \rho_{12})/(\rho_{12}^2 - \rho_{11}\rho_{22}),\\
S_2 &= (\rho_{11} + 2\rho_{12} + \rho_{22})/(\rho_{12}^2 - \rho_{11}\rho_{22}).
\end{aligned}$$

The coefficient ρ_{11}, ρ_{12} and ρ_{22} have the following relations:

$$\rho_{11} + \rho_{12} = (1-\phi)\rho_{\mathrm{s}}, \tag{3a}$$

$$\rho_{12} + \rho_{22} = \phi\rho_{\mathrm{f}}, \tag{3b}$$

where ρ_{s} and ρ_{f} are the density of the solid material and the fluid, respectively.

3. Stiffness problems

Carcione and Quiroga-Goode[12] discussed the eigenvalues of the propagation matrix of Biot's poroacoustic equations in a low-frequency range. In their work, it is shown that the eigenvalues come out of complex conjugates. The eigenvalues of the propagation matrix have negative real parts and are different greatly in magnitude due to the viscous term. The presence of this large eigenvalue together with small eigenvalues indicates that the problem is stiff. For numerical stability, the domain of convergence of the time integration scheme should include this large

eigenvalue.[14] For Biot's equations, the stability condition of the staggered-grid FD algorithm often used is[17]

$$\mathrm{d}t \leq h \Big/ \sqrt{v_{\mathrm{p}}^{\mathrm{f}2} + v_{\mathrm{s}}^2}, \tag{4}$$

where $\mathrm{d}t$ is the time step; h is the grid interval in both the x- and z- axis; $v_{\mathrm{p}}^{\mathrm{f}}$ is the fast wave, and v_{s} is the shear wave velocity. Equation (4) is obtained by generalizing the stability condition for the elastic FD scheme. However, a rigorous stability condition for Biot's equations in staggered grid FD algorithms has not been obtained due to the complexity of dispersion equation. In the numerical modelling of wave propagation in porous media, Eq.(4) is valid when the damping coefficient b is small. However, when b is relatively large, the simulation will be unstable, even though Eq.(4) is satisfied. The key factor leading to this problem is that the slow wave has very low velocity, and even becomes static. In the following part, we will perform the stability analysis, and then give the stability condition required in the staggered FD algorithm for modelling elastic wave propagation in general porous elastic media.

For simplicity, in one dimension, Eqs.(1) and (2) in a staggered grid can be written as ($\mu = 0$ in one dimension)

$$v_x^{\mathrm{s}n+1/2} = v_x^{\mathrm{s}n-1/2} + bR_3\mathrm{d}tv_x^{\mathrm{f}n-1/2} - R_2\mathrm{d}t\delta_x\sigma_{xx}^n + R_1\mathrm{d}t\delta_x\sigma^n, \tag{5a}$$

$$v_x^{\mathrm{f}n+1/2} = v_x^{\mathrm{f}n-1/2} + bS_2\mathrm{d}tv_x^{\mathrm{f}n-1/2} - R_3\mathrm{d}t\delta_x\sigma_{xx}^n + S_1\mathrm{d}t\delta_x\sigma^n, \tag{5b}$$

$$\sigma_{xx}^{n+1} = \sigma_{xx}^n + (A+Q)\mathrm{d}t\delta_x v_x^{\mathrm{s}n+1/2} - Q\mathrm{d}t\delta_x v_x^{\mathrm{f}n+1/2}, \tag{5c}$$

$$\sigma^{n+1} = \sigma^n + (Q+R)\mathrm{d}t\delta_x v_x^{\mathrm{s}n+1/2} - R\mathrm{d}t\delta_x v_x^{\mathrm{f}n+1/2}. \tag{5d}$$

In the above equations, the superscripts denote the time step. δ_x is the derivative operator with respect to x in the x- direction. For the case of plane wave solution, the derivative operator, using finite difference method for computing the spatial derivatives, is denoted by[18]

$$\delta_x = \frac{2\mathrm{i}}{\mathrm{d}x}\sum_{m=0}^{N-1} a_m \sin\left(k_x\frac{2m+1}{2}\mathrm{d}x\right),$$

where $\mathrm{d}x$ is the spatial step, k_x is the wave number along the x-direction, N is the derivative operator length, and a_m are the weighted-derivative coefficients which have different values for different N.[19]

The following matrix equation for the Eq.(5) is obtained in matrix form:

$$V^{n+1/2} = B_1V^{n-1/2} + B_2V^n, \tag{6}$$

where

$$V^{n+1/2} = (v_x^{\mathrm{s}n+1/2}, v_x^{\mathrm{f}n+1/2}, \sigma_{xx}^{n+1}, \sigma^{n+1})^{\mathrm{T}},$$
$$V^n = (v_x^{\mathrm{s}n+1/2}, v_x^{\mathrm{f}n+1/2}, \sigma_{xx}^n, \sigma^n)^{\mathrm{T}},$$
$$V^{n-1/2} = (v_x^{\mathrm{s}n-1/2}, v_x^{\mathrm{f}n-1/2}, \sigma_{xx}^n, \sigma^n)^{\mathrm{T}},$$

and

$$B_1 = \begin{bmatrix} 1 & bR_3\mathrm{d}t & 0 & 0 \\ 0 & 1+bS_2\mathrm{d}t & 0 & 0 \\ 0 & 0 & 1 & 0 \\ 0 & 0 & 0 & 1 \end{bmatrix},$$

$$B_1 = \begin{bmatrix} 0 & 0 & -R_2\mathrm{d}t\delta_x & R_1\mathrm{d}t\delta_x \\ 0 & 0 & -R_3\mathrm{d}t\delta_x & S_1\mathrm{d}t\delta_x \\ (A+Q)\mathrm{d}t\delta_x & -Q\mathrm{d}t\delta_x & 0 & 0 \\ (Q+R)\mathrm{d}t\delta_x & -R\mathrm{d}t\delta_x & 0 & 0 \end{bmatrix}.$$

The above matrix equation can be written alternatively as

$$U^{n+1} = SU^n, \tag{7}$$

where

$$U^{n+1} = \begin{pmatrix} V^{n+1} \\ V^{n+1/2} \end{pmatrix}, \quad U^n = \begin{pmatrix} V^{n+1/2} \\ V^n \end{pmatrix},$$

and

$$S = \begin{pmatrix} B_2 & B_1 \\ \mathrm{I} & O \end{pmatrix},$$

where matrix I is the identity matrix of 4×4 order, and matrix O is the zero matrix of 4×4 order.

Usually, the stability analysis is related to the Von Neumann stability criterion. Based on the von Neumann condition, the eigenvalue of the matrix S should not be larger than 1, i.e. the absolute eigenvalue is[20]

$$|\lambda| \leq 1. \tag{8}$$

The formula for calculating the eigenvalues of the matrix S can be written as

$$|S - \lambda I_1| = 0, \tag{9}$$

where I_1 is the identity matrix of 8×8 order. Then we have

$$\lambda^4 \left| B_2 - \lambda I + \frac{B_1}{\lambda} \right| = 0. \tag{10}$$

The largest negative eigenvalue corresponds to the slow wave for the case of the wave number $k = 0$.[12,14] Thus when $k_x = 0$, we have

$$\lambda^4 \left(\frac{1}{\lambda} - \lambda \right)^3 \left[\frac{1}{\lambda}(1 + bS_2 \mathrm{d}t) - \lambda \right] = 0. \tag{11}$$

For satisfying the stability condition given by Eq.(8), the following inequality should hold:

$$|\sqrt{1 + bS_2 \mathrm{d}t}| \leq 1 \quad \text{or} \quad bS_2 \mathrm{d}t \geq -2. \tag{12}$$

Equation (12) implies that a small time step dt should be used in order to keep the numerical solutions stable. The larger the value of b is, the smaller the value of dt should be. When the permeability of a reservoir rock is very small and the viscosity of pore fluid is relatively large, especially for modelling oil-bearing reservoirs, the numerical algorithm needs a rather small dt. This will occupy much computer memory and take huge computation time and iterations.

4. Implementation of the partition method

The problem introduced by the stiffness of Biot's poroelastic system is solved by using a partition method as was done by Carcione and Quiroga-Goode.[12] The idea is to partition a stiff system into a small stiff system and a large nonstiff system, so that the two systems can be treated by two different methods, one is implicit, and the other is explicit. In this work, we solve the former analytically, while for the latter, we use the high-order stagger-grid finite difference method.[4] In this case, the stiff equations are

$$\dot{v}_i^{\mathrm{s}} = bR_3 v_i^{\mathrm{f}}, \tag{13a}$$

$$\dot{v}_i^{\mathrm{f}} = bS_2 v_i^{\mathrm{f}}. \tag{13b}$$

For the above equations, we can obtain the analytical solutions in two dimensions in an x-z plane, i.e.

$$\dot{v}_x^{\mathrm{s}'} = v_x^{\mathrm{s}^0} + \frac{R_3}{S_2}[\exp(bS_2 t) - 1] v_x^{\mathrm{f}^0}, \tag{14a}$$

$$\dot{v}_z^{\mathrm{s}'} = v_z^{\mathrm{s}^0} + \frac{R_3}{S_2}[\exp(bS_2 t) - 1] v_z^{\mathrm{f}^0}, \tag{14b}$$

$$v_x^{\mathrm{f}'} = v_x^{\mathrm{f}^0} \exp(bS_2 t), \tag{14c}$$

$$v_z^{\mathrm{f}'} = v_z^{\mathrm{f}^0} \exp(bS_2 t). \tag{14d}$$

We define the following intermediate vector as the input for an explicitly high-order staggered-grid FD in an eighth-order accuracy in space and a second-order accuracy in time, i.e.

$$V' = (v_x^{\mathrm{s}'}, v_z^{\mathrm{s}'}, v_x^{\mathrm{f}'}, v_z^{\mathrm{f}'}, \sigma_{xx}, \sigma_{zz}, \sigma_{xz}, \sigma)^{\mathrm{T}}. \tag{15}$$

For the two dimensional situation, in a staggered grid, the nonstiff FD equations can be written as

$$v_{x(i+1/2,j)}^{\mathrm{s}(n+1/2)} = v_x^{\mathrm{s}'} - R_2 \mathrm{d}t D_x \sigma_{xx(i+1/2,j)}^{(n)} - R_2 \mathrm{d}t D_z \sigma_{xz(i+1/2,j)}^{(n)} + R_1 \mathrm{d}t D_x \sigma_{(i+1/2,j)}^{(n)}, \tag{16a}$$

$$v_{z(i,j+1/2)}^{\mathrm{s}(n+1/2)} = v_z^{\mathrm{s}'} - R_2 \mathrm{d}t D_x \sigma_{xz(i,j+1/2)}^{(n)} - R_2 \mathrm{d}t D_z \sigma_{zz(i,j+1/2)}^{(n)} + R_1 \mathrm{d}t D_z \sigma_{(i,j+1/2)}^{(n)}, \tag{16b}$$

$$v_{x(i+1/2,j)}^{\mathrm{f}(n+1/2)} = v_x^{\mathrm{f}'} - R_3 \mathrm{d}t D_x \sigma_{xx(i+1/2,j)}^{(n)} - R_3 \mathrm{d}t D_z \sigma_{xz(i+1/2,j)}^{(n)} + S_1 \mathrm{d}t D_x \sigma_{(i+1/2,j)}^{(n)}, \tag{16c}$$

$$v_{z(i,j+1/2)}^{\mathrm{f}(n+1/2)} = v_z^{\mathrm{f}'} - R_3 \mathrm{d}t D_x \sigma_{xz(i,j+1/2)}^{(n)} - R_3 \mathrm{d}t D_z \sigma_{zz(i,j+1/2)}^{(n)} + S_1 \mathrm{d}t D_z \sigma_{(i,j+1/2)}^{(n)}, \tag{16d}$$

and

$$\begin{aligned} \sigma_{xx(i,j)}^{(n+1)} = \sigma_{xx(i,j)}^{(n)} &+ (2\mu + A + Q)\mathrm{d}t D_x v_{x(i,j)}^{\mathrm{s}(n+1/2)} + (A + Q)\mathrm{d}t D_z v_{z(i,j)}^{\mathrm{s}(n+1/2)} \\ &- Q\mathrm{d}t \left(D_x v_{x(i,j)}^{\mathrm{f}(n+1/2)} + D_z v_{z(i,j)}^{\mathrm{f}(n+1/2)} \right), \end{aligned} \tag{17a}$$

$$\begin{aligned} \sigma_{zz(i,j)}^{(n+1)} = \sigma_{zz(i,j)}^{(n)} &+ (A + Q)\mathrm{d}t D_x v_{x(i,j)}^{\mathrm{s}(n+1/2)} + (2\mu + A + Q)\mathrm{d}t D_z v_{z(i,j)}^{\mathrm{s}(n+1/2)} \\ &- Q\mathrm{d}t \left(D_x v_{x(i,j)}^{\mathrm{f}(n+1/2)} + D_z v_{z(i,j)}^{\mathrm{f}(n+1/2)} \right), \end{aligned} \tag{17b}$$

$$\sigma_{xz(i+1/2,j+1/2)}^{(n+1)} = \sigma_{xz(i+1/2,j+1/2)}^{(n)} + \mu \mathrm{d}t \left(D_x v_{z(i+1/2,j+1/2)}^{\mathrm{s}(n+1/2)} + D_z v_{x(i+1/2,j+1/2)}^{(\mathrm{s})(\mathrm{n}+1/2)} \right), \tag{17c}$$

$$\sigma_{(i,j)}^{(n+1)} = \sigma_{(i,j)}^{(n)} + (Q + R)\mathrm{d}t \left(D_x v_{x(i,j)}^{\mathrm{s}(n+1/2)} + D_z v_{z(i,j)}^{\mathrm{s}(n+1/2)} \right) - R\mathrm{d}t \left(D_x v_{x(i,j)}^{\mathrm{f}(n+1/2)} + D_z v_{z(i,j)}^{\mathrm{f}(n+1/2)} \right). \tag{17d}$$

In Eqs.(16) and (17), the superscripts represent the time step and the subscripts denote the spatial indices. The distributions of stress, particle velocity and material parameters for staggered grid finite difference algorithm are shown in Fig.1.

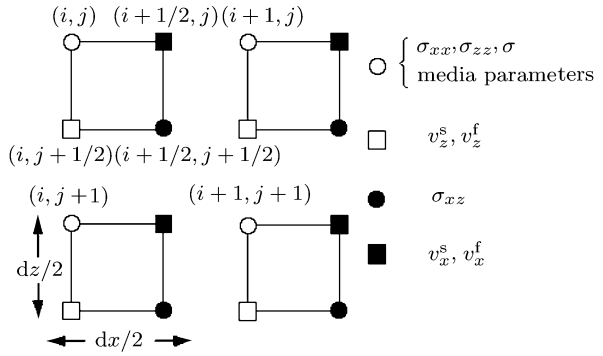


Fig.1. The relative locations of physical variable components in a staggered-grid formulation.

According to the staggered FD algorithm in time and space domains, the formulations for the derivatives of stress and particle velocity components, for example, for $D_x\sigma_{xx}$ and $D_x v_z^{\rm s}$, are

$$D_x\sigma^{(n)}_{xx(i+1/2,j)} = \frac{1}{\mathrm{d}x}\sum_{n=0}^{N-1} a_m \left[\sigma^{(n)}_{xx(i+m+1,j)} - \sigma^{(n)}_{xx(i-m,j)}\right], \tag{18a}$$

$$D_z\sigma^{{\rm s}(n+1/2)}_{z(i,j)} = \frac{1}{\mathrm{d}z}\sum_{n=0}^{N-1} a_m \left[v^{{\rm s}(n+1/2)}_{z(j,j+m+1/2)} - v^{{\rm s}(n+1/2)}_{z(i,j-m-1/2)}\right], \tag{18b}$$

where $\mathrm{d}x$ and $\mathrm{d}z$ are the space steps along the x- and z- directions, respectively. In this paper, N is taken as 4, namely, the staggered algorithm possesses an eighth-order accuracy in space.

5. Numerical modelling and comparisons

In our work, the time function of the source is the first derivative of a Gaussian function, i.e.

$$s(t) = (t-t_0)\mathrm{e}^{-[\pi f_0(t-t_0)]^2}, \tag{19}$$

where f_0 is the dominant frequency, and t_0 is the central time of the time function. A bulk source is used in this paper. The source energy is partitioned linearly between the solid and the fluid phases as is done in Ref.[17].

The credibility of the numerical simulation by using our proposed method can be verified by comparing the numerical results with the analytical solutions. We use analytical solution derived by Dai[21] for Biot's equations in a homogeneous, poroelastic medium filled with a fluid. The analytical solution does not take into account the viscosity effect, i.e. the damping coefficient b is zero. The material properties and Biot's parameters are chosen as follows: the apparent density $\rho_{12} = -83\,\mathrm{kg/m^3}$; the solid density $\rho_{\rm s} = 2500\,\mathrm{kg/m^3}$; the fluid density $\rho_{\rm f} = 104\,\mathrm{kg/m^3}$; the medium porosity $\phi = 0.2$; the solid modulus $K_{\rm s} = 40\,\mathrm{GPa}$; the matrix bulk modulus $K_m = 20\,\mathrm{GPa}$; the fluid bulk modulus $K_{\rm f} = 2.5\,\mathrm{GPa}$; the viscosity $\eta = 0.001\,\mathrm{Nsm^2}$; and the permeability $\kappa = 6\times10^{-13}\,\mathrm{m^2}$. During the numerical calculation, the size of the model is 600 m by 600 m, with $\mathrm{d}x = \mathrm{d}z = 2\,\mathrm{m}$, respectively, and $\mathrm{d}t = 0.1\,\mathrm{ms}$. A P-wave line source is located at the position (300 m, 300 m) with a dominant frequency of 50 Hz, and the receiver is positioned at the position (220 m, 220 m). The grid point number per minimum wavelength is 3 approximately, namely $v_{\rm p}^{\rm s}/\mathrm{d}x \cdot f_{\rm high} \approx 3$, where $v_{\rm p}^{\rm s}$ is the velocity of the slow wave, and $f_{\rm hifh}$ is referred to as the high frequency of the source. We can analytically calculate $v_{\rm p}^{\rm f} = 4260\,\mathrm{m/s}$ and $v_{\rm p}^{\rm s} = 1210\,\mathrm{m/s}$. The solution at the receiver is calculated numerically and analytically, separately, and the calculated results are shown in Fig.2. From Fig.2, we see that the numerical solution coincides with the analytical solution very well.

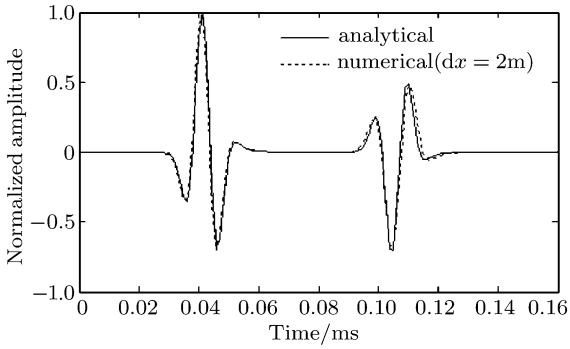


Fig.2. Comparisons of the analytical solution and the numerical solution in our proposed partition method. Waveforms for the vertical particle velocity component in the solid are calculated; the numerical solution is shown by a dotted line, and the analytical solution by a solid line, with the viscosity being zero.

We also compare two numerical solutions, one by using the non-partition (normal) staggered-grid FD, and another by using the staggered-grid FD with the partition method. In Fig.3, (a) is for the case of $\eta = 0$, and (b) for $\eta \neq 0$. Biot's parameters are the same as

those used in Fig.2. The dominant frequency of the source is 300 Hz. The space step $\mathrm{d}x = \mathrm{d}z$ =0.2 m, and the time step $\mathrm{d}t$ = 0.01 ms. The size of the model is 60 m by 60 m. The source is located at the centre of the model, while the receiver is placed at the position (38 m, 22 m). Apparently, the two numerical solutions match perfectly for both cases of $\eta = 0$ and $\eta \neq 0$. When the permeability of the porous media is taken as $6 \times 10^{-14}\,\mathrm{m}^2$, in the normal FD method occurs a numerical instability. While the partitioned FD method does a good job and effectively completes the numerical simulation. Alternatively, we may use the smaller time step in the normal FD method to avoid the instability, but it will take more computing time.

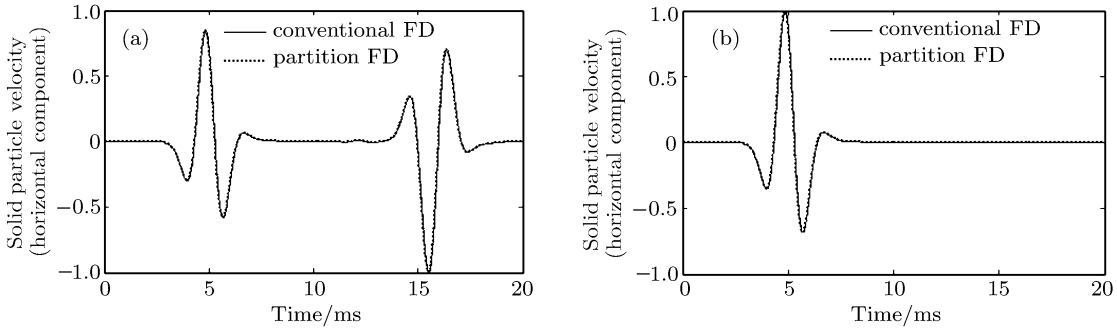


Fig.3. Waveform comparison between the solutions obtained by using the conventional FD algorithm (solid line) and the partition FD method (dotted line) with $\eta = 0$ (a) and $\eta \neq 0$ (b), respectively.

For observing the characteristics of the slow wave propagating in a porous medium, we perform a modelling test for a 2D homogeneous porous model. The size of the model is 600 m × 600 m. A pure compressional line source is placed at the centre of the model with a dominant frequency 30 Hz. The space step is 2 m for both x- and z-direction, respectively, and the time step is 0.2 ms. The porous model has the following parameters: $\rho_\mathrm{s} = 2500\,\mathrm{kg/m^3}$, $\rho_\mathrm{f} = 1040\,\mathrm{kg/m^3}$, $\eta = 0.001\,\mathrm{Nsm^2}$, $\kappa = 6 \times 10^{-11}\,\mathrm{m^2}$, $\phi = 0.2$, $v_\mathrm{p}^\mathrm{f} = 3200\,\mathrm{m/s}$, v_s=1558 m/s, $v_\mathrm{f} = 1550\,\mathrm{m/s}$. In this case, the damping coefficient b has the value of $6.7 \times 10^5\,\mathrm{Ns/m^4}$. The apparent density ρ_{12} can be obtained by $\rho_{12} = \phi\rho_\mathrm{f}(1-\alpha)$. α is the tortuosity which is related to the porosity, i.e. $\alpha = 1 + r_\mathrm{c}(1-\phi)/\phi$, where r_c is a constant with a value between 0 and 1. And $r_\mathrm{c} = 0.5$ is used in numerical modelling, which corresponds to spherical grains.[22] The permeability κ is taken as being relatively large for the purpose of observing the characteristics of slow waves. As can be seen in Figs.4 and 5, the slow waves are diffusive and appear as static modes at the source location.

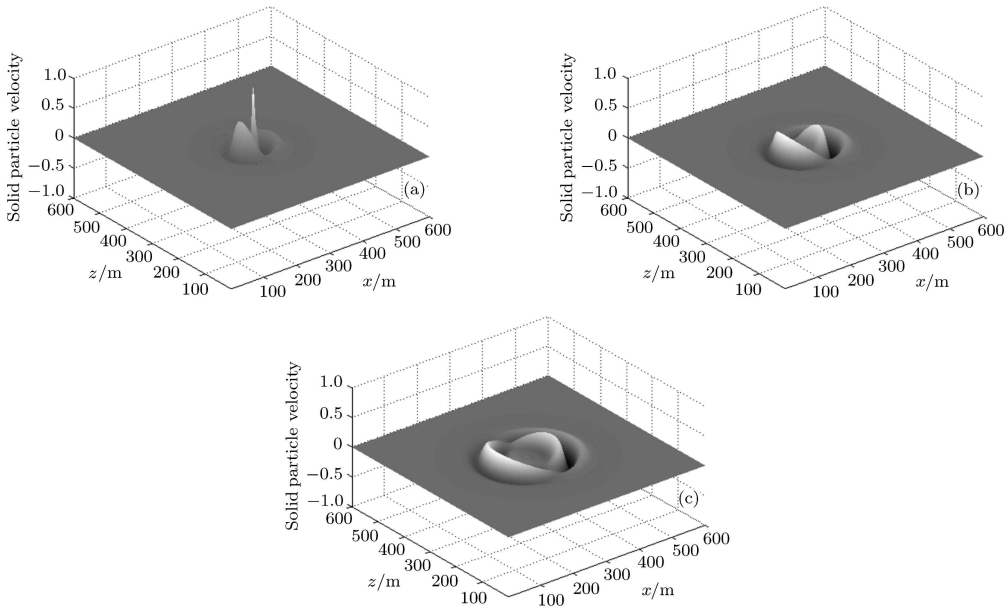


Fig.4. Snapshots of the horizontal components for solid particle-velocity at 0.03 s (a), 0.04 s (b), and 0.05 s (c), respectively. The amplitudes are scaled with respect to the absolute maximum value of the wave amplitude at 0.03 s.

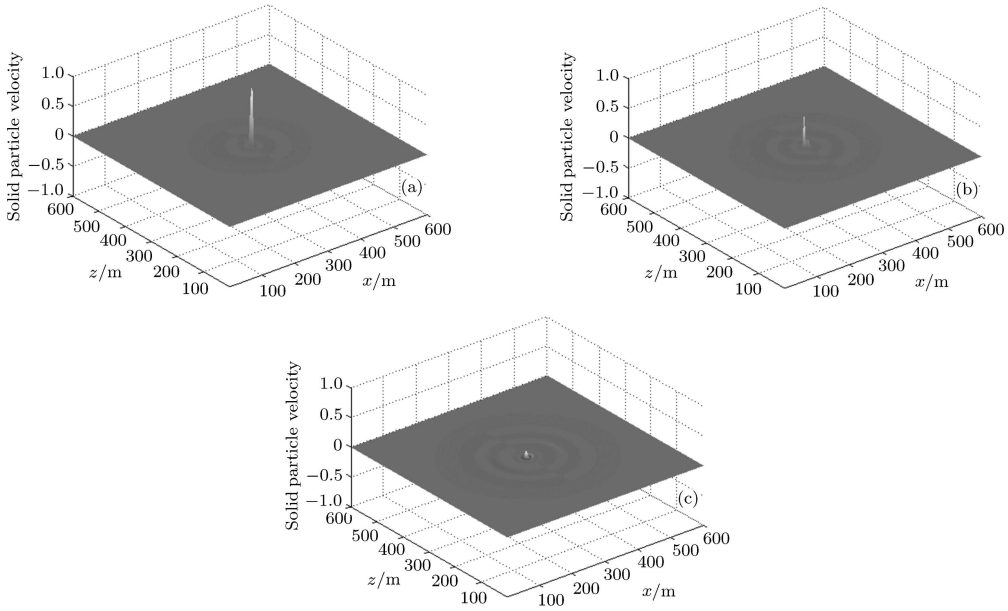


Fig.5. Snapshots of the horizontal components for fluid particle-velocity at 0.03 s (a), 0.04 s (b), and 0.05 s (c), respectively. The amplitudes are scaled with respect to the absolute maximum value of the wave amplitude at 0.03 s.

The slow waves with their solid particle-velocity components attenuate more rapidly than those with their fluid particle velocity components.

In this numerical example, slow waves cannot propagate properly because their velocities are nearly zero. For most of situations, they cannot be observed normally in typical oil bearing reservoirs. However, they carry out part of energy and attenuate quickly. What is more, when heterogeneous media are taken into account, fast waves or shear waves can be converted into slow waves at interfaces. These waves should be taken into account in evaluating wave attenuation.

In order to demonstrate the capability of our proposed high-order staggered-grid FD in the partition method, we consider a relatively complex model in seismic exploration for performing a numerical test, as seen in Fig.6. The width and the length of the model are both 4 km. A pure compressional line source is located at the position (2 km, 1 km), with a dominant frequency being 10 Hz. A receiver array is placed across the source location and parallel to the x-direction. The material parameters of the numerical model are given in Table 1. For the parameters of the discretization, $\mathrm{d}x = \mathrm{d}z = 10\,\mathrm{m}$, and $\mathrm{d}t = 0.8\,\mathrm{ms}$. The common shot gathers, i.e. the waveforms collected by these receivers with this single source, are given in Fig.7.

Table 1. Parameters of layered medium model.

Parameter	Layer1	Layer2	Layer3
$\rho_\mathrm{s}/\mathrm{kg\cdot m^{-3}}$	2300	2500	2800
$\rho_\mathrm{f}/\mathrm{kg\cdot m^{-3}}$	1000	1000	1030
$v_\mathrm{p}^\mathrm{f}/\mathrm{m\cdot s^{-1}}$	3000	3500	4100
$v_\mathrm{s}/\mathrm{m\cdot s^{-1}}$	1732	2021	2367
$v_\mathrm{f}/\mathrm{m\cdot s^{-1}}$	1500	1500	1550
$\phi/\%$	35	18	10
$\kappa/10^{-13}\mathrm{m}^2$	6	4	1
$\eta/\mathrm{Pa\cdot s}$	0.001	0.002	0.005

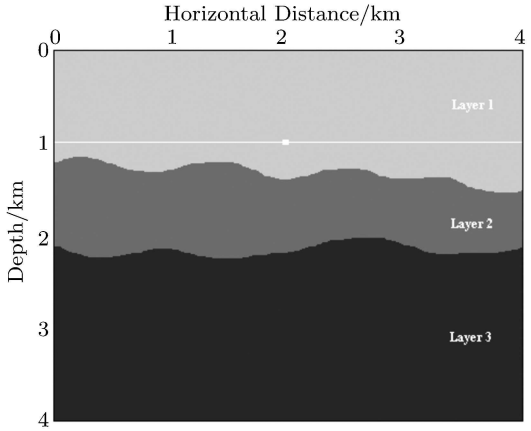


Fig.6. The 2D model with 4 km by 4 km in horizontal and vertical directions, respectively in which there are three layers. The source is located at the positions (2 km, 1 km), denoted by a white spot. The receiver array is located horizontally across the source, denoted by a white line.

Figure 7(a) is for the equivalent elastic case, while Figs.7(b) and 7(c) are for the porous elastic ($b \neq 0$) and porous elastic ($b = 0$) cases, respectively. During the numerical computation, based on our previous work, the PML method is applied as an absorbing boundary condition to reduce spurious reflections from the artificial boundaries.[16] For the given material parameters, the conventional staggered-grid FD scheme will be unstable unless the time step is taken as being very small (not larger than 2.2 μs, according to the stability condition (12)). By using the partition method, for a large value b, we can choose a coarse time step determined only by the numerical algorithm that solves the nonstiff equations. In Fig.7, it is seen that the common shot gathering of the equivalent elastic model is almost the same as that of the porous elastic model with $b \neq 0$, except that the reflected waves attenuate more rapidly for the latter model than for the former model. In addition, Figure 7(c) shows some converted waves that are produced due to porous elastic effects and cannot be observed in Figs.7(a) and 7(b). In a seismic frequency range, the slow wave cannot be observed generally as shown in Fig.7(b), and their strong attenuation precludes the slow wave from propagating in practice.

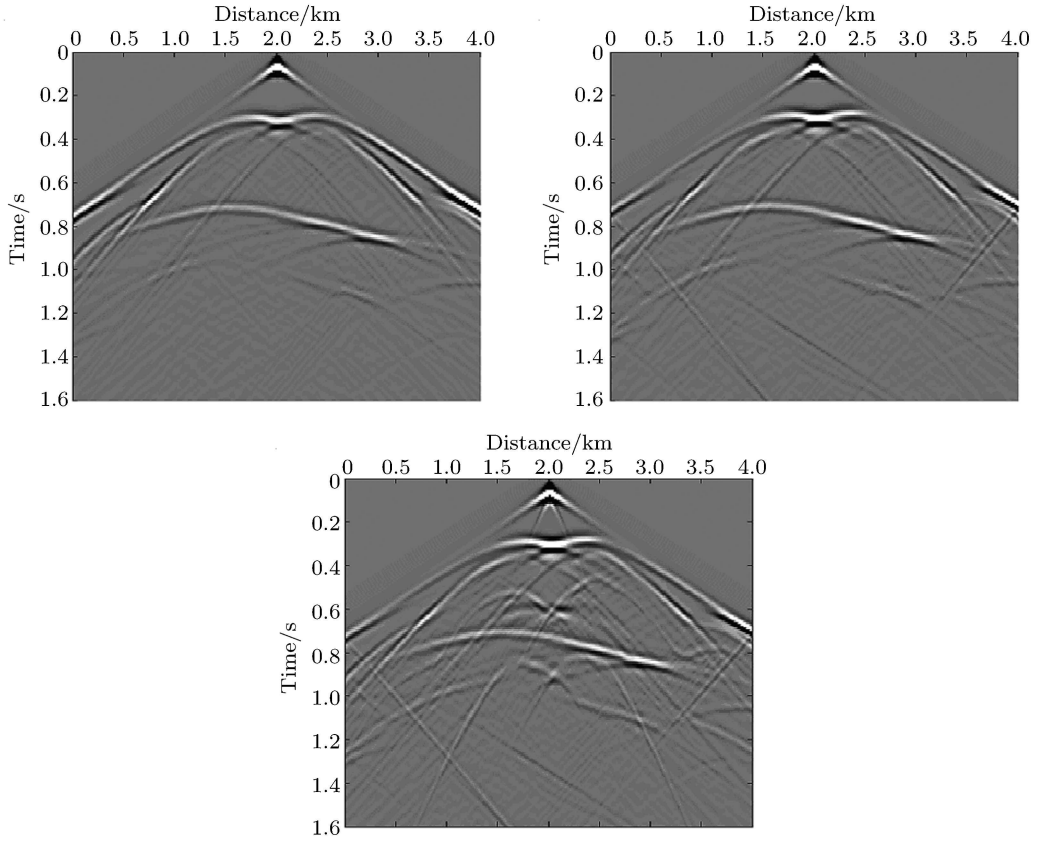


Fig.7. The common shot gathers of the vertical particle-velocity component of the solid for the equivalent elastic (a), porous elastic with $b \neq 0$ (b), and porous elastic with $b = 0$ (c) models, respectively. The model parameters are shown in Table 1. An explosive compressional source is used with a dominant frequency of 10 Hz.

6. Conclusions and discussion

Biot's dynamical equations describing wave propagation in a porous medium filled with a fluid are stiff when the fluid viscosity is not zero and the permeability of a reservoir rock is small. A partition method developed in our work is used to solve the stiffness problem of Biot's poroelastic equations in our staggered high-order finite-difference scheme. Therefore, Biot's system is divided into two parts. One is stiff and can be solved analytically, and the other is nonstiff and can be solved by using a high-order staggered-grid finite-difference method. The algorithm has a second-order accuracy in time and an eighth-order accuracy in space.

Our algorithm has been compared with the ana-

lytical solution and the conventional FD scheme, and they are in good agreement. Using our proposed method, the time step can be determined only by the nonstiff equations, which greatly reduces the calculation time iterations by a factor of hundred (even thousand) in stable calculations.

In our simulation, we have observed the static mode and diffusive characteristic of slow waves. The numerical modelling also shows that the slow wave and its static mode are stronger for the fluid particle-velocities than for the solid ones. Because of its high attenuation in a seismic frequency range, the wave propagation in porous elastic media has the similar character to that in equivalent elastic media. The ratio between the fluid viscosity and the medium permeability affects the attenuation and the velocity of the slow P wave greatly. By using the partition method, we can simulate more realistic media having a large viscosity and low permeability in a low frequency range.

References

[1] Schmitt D P 1989 *J. Acoust. Soc. Am.* **86** 2397

[2] Carcione J M and Quiroga-Goode G 1996 *Geophys. Prospect.* **44** 99

[3] Diallo M S and Appel E 2000 *J. Appl. Geophys.* **44** 313

[4] Wang X M, Zhang H L and Wang D 2003 *Chin. J. Geophys.* **46** 842

[5] Hu H S 2003 *Acta Phys. Sin.* **52** 1954 (in Chinese)

[6] Biot M A 1956 *J. Appl. Mech.* **23** 91

[7] Biot M A 1956 *J. Acoust. Soc. Am.* **28** 168

[8] Biot M A 1962 *J. Appl. Phys.* **3** 1482

[9] Stoll R D 1979 *J. Acoust. Soc. Am.* **66** 1152

[10] Dvorkin J and Nur A 1993 *Geophysics* **58** 524

[11] Carcione J M 1998 *Geophys. Prospect.* **46** 249

[12] Carcione J M and Quiroga-Goode G 1995 *J. Comput. Acoust.* **3** 261

[13] Willard L M 1981 *Numerical Methods for Stiff Equations and Singular Perturbation Problems* (Holland: Reidel)

[14] Carcione J M 1996 *J. Acoust. Soc. Am.* **99** 2655

[15] Zhao H B, Wang X M and Zhang H L 2005 *IEEE Ultrasonic Symposium* **3** 1472

[16] Zhao H B, Wang X M, Wang D and Chen H 2006 *Chin. J. Geophys.* (accepted)

[17] Zhu X and McMechan G A 1991 *Geophysics* **56** 328

[18] Zhang H L, Wang X M and Zhang B X 2004 *Acoustic Field and Wave in Borehole* (Beijing: Science Press)

[19] Wang X M 2001 *The* 5*th SEGJ International Symposium of Imaging Technology* Tokyo 113

[20] Durran D R 1999 *Numerical Methods for Wave Equations in Geophysical Fluid Dynamics* (New York: Springer)

[21] Dai N, Vafidis A and Kanasewich E R 1995 *Geophysics* **60** 327

[22] Berryman J G. 1981 *J. Acoust. Soc. Am.* **69** 416